

# Efficient generation of cross-polarized femtosecond pulses in cubic crystals with holographic cut orientation

Lorenzo Canova,<sup>1</sup> Stoyan Kourtev,<sup>2</sup> Nikolay Minkovski,<sup>2</sup> Aurélie Jullien,<sup>1</sup> Rodrigo Lopez-Martens,<sup>1</sup> Olivier Albert,<sup>1</sup> and Solomon M. Saltiel<sup>2,a)</sup>

<sup>1</sup>Laboratoire d'Optique Appliquée, ENSTA, Ecole Polytechnique, CNRS UMR-7639, 91761 Palaiseau Cedex, France

<sup>2</sup>Physics Department, Sofia University, Sofia-1164, Bulgaria

(Received 1 May 2008; accepted 16 May 2008; published online 9 June 2008)

We report here an alternative and more efficient orientation of cubic crystals for generation of cross-polarized femtosecond laser pulses. We show both theoretically and experimentally that the cross polarized wave generation (XPWG) is more efficient when the fundamental beam propagates along the [011] direction (holographic cut) in the crystal than along the [001] direction previously reported. With the [011]-cut BaF<sub>2</sub> crystal we measured the highest XPWG conversion efficiencies. We prove other very important advantages of the [011]-cut approach: weak induced phase mismatch and no need for its compensation. © 2008 American Institute of Physics. [DOI: 10.1063/1.2939584]

Cross-polarized-wave generation (XPWG) has demonstrated its capacity to increase the temporal contrast of high intensity femtosecond pulses.<sup>1,2</sup> The results published so far on XPWG relied exclusively on the use of z-cut crystals ([001] orientation). The main drawback of this z-cut crystal orientation scheme is its sensitivity to the input polarization orientation at high intensities. Whether one wants to directly use the XPW beam or reamplify it in a double chirp pulse amplification (CPA) femtosecond laser scheme, it is natural to look for new approaches to increase the intrinsic efficiency of the XPW process.

The XPWG is a third order nonlinear optical effect that can be classified as four wave mixing process degenerate with respect to all frequencies and nondegenerate with respect to the polarization vectors of the interacting waves. As a result an output wave polarized perpendicularly to the input one is generated via  $\omega_{\perp} = \omega_{\parallel} + \omega_{\parallel} - \omega_{\parallel}$  process. For cubic crystals (*m3m*) the efficiency of the XPWG depends on the product of the  $\chi_{xxxx}^{(3)}$  component, the crystal length *L*, the input intensity, and the anisotropy of  $\chi^{(3)}$ -tensor  $\sigma = [\chi_{xxxx}^{(3)} - 3\chi_{xyyy}^{(3)}] / \chi_{xxxx}^{(3)}$ .<sup>3-6</sup> The XPWG is automatically phase matched, but for z-cut samples at high intensities, self-phase and cross-phase modulation brake the exact phase matching which leads to saturation in the efficiency. This induced phase mismatch can be compensated by changing orientation of input polarization.<sup>3</sup>

Z-cut crystal orientation for XPWG in BaF<sub>2</sub> crystals was an academic choice aimed at demonstrating the feasibility of the XPW filtering. In Ref. 3 the YVO<sub>4</sub> crystal has been investigated as a XPW generator with pumping along the Z axis. Although the nonlinearity is higher, the maximum achievable efficiency is the same. In addition, because of its linear birefringence, a very accurate crystal alignment is mandatory in order to avoid degradation in the input polarization. There are no reports about other crystals suitable for XPWG. Another solution is to explore more efficient orientations in cubic crystals.

Consequently, we performed a theoretical analysis of the XPWG efficiency for arbitrary orientations of the fundamen-

tal beam (FB). This analysis shows that for cubic crystals the holographic cut ensures the highest efficiency with the added advantage that the position of optimal FB polarization is less sensitive to changes in the input intensity. The purposes of this letter are: (i) to present the experimental results for XPWG with [011]-cut samples showing increase in efficiency; (ii) to show the advantage of holographic cut crystals as XPW generators, which is decreased sensitivity to the orientation of FB polarization at high intensity; and (iii) to report the coupling coefficients of the equations describing XPWG in [011] direction. Where possible, we present comparisons with the results of XPWG obtained with z-cut crystals.

The schematic of the setup with single nonlinear crystal (NLC) with *m3m* symmetry situated between crossed polarizers is shown in Fig. 1(a). The system of two plane wave equations for the two interacting waves which describes the

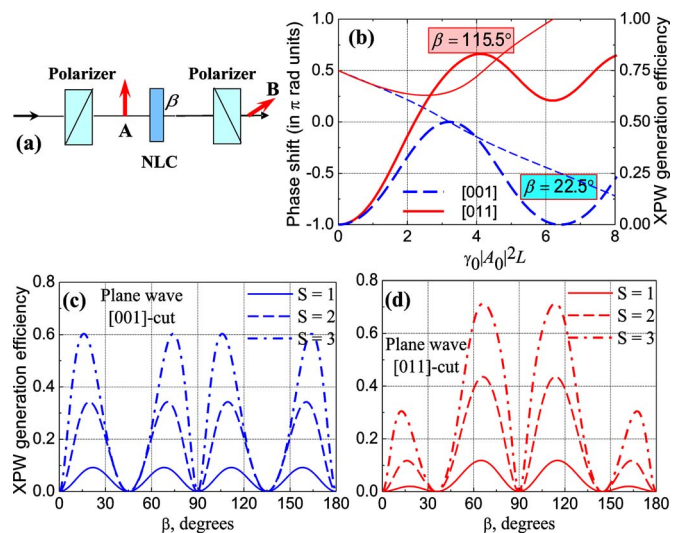


FIG. 1. (Color online) (a) Schematic of the XPWG experiment. (b) Comparison of plane-wave XPWG efficiencies for the two cuts (right scale-thick lines). Comparison of the phase shift between fundamental wave and XPW for the two cuts (left scale-thin lines). [(c) and (d)] XPWG efficiency as a function of angle  $\beta$  for different normalized input intensities for [001]-cut (c) and for [011]-cut (d). For all curves  $\sigma = -1.2$  (Ref. 3).  $S = \gamma_0 |A_0|^2 L$ .

<sup>a)</sup>Electronic mail: saltiel@phys.uni-sofia.bg.

TABLE I. Nonlinear coupling coefficients used in Eqs (1) and (2) for both  $z$ -cut and holographic cut.  $D$  stands for  $D=1+(3\sigma/16)\cos 4\beta-7\sigma/16$ ,  $\gamma_0=6\pi\chi_{xxxx}^{(3)}/8n\lambda$ .

	$z$ -cut	Holographic cut
$\gamma_1$	$\gamma_0[1-(\sigma/2)\sin^2(2\beta)]$	$\gamma_0[D-(\sigma/4)\cos 2\beta]$
$\gamma_2$	$-(\gamma_0\sigma/2)\sin 2\beta\cos 2\beta$	$-(\gamma_0\sigma/8)\sin 2\beta(3\cos 2\beta-1)$
$\gamma_3$	$(\gamma_0/3)(4-\sigma)-\gamma_1$	$(\gamma_0/3)[D-(3\sigma/4)\cos 4\beta]$
$\gamma_4$	$-\gamma_2$	$(\gamma_0\sigma/8)\sin 2\beta(3\cos 2\beta+1)$
$\gamma_5$	$\gamma_1$	$\gamma_0[D+(\sigma/4)\cos 2\beta]$
$\beta_{\text{zero}}$	$0^\circ; 45^\circ; 90^\circ; 135^\circ; 180^\circ$	$0^\circ; 35.3^\circ; 90^\circ; 144.7^\circ; 180^\circ$

XPWG in cubic crystals has the following form.<sup>3</sup>

$$-i\frac{dA}{d\xi} = \gamma_1 AA^*A + \gamma_2 AAB^* + 2\gamma_2 AA^*B + 2\gamma_3 AB^*B + \gamma_3 BBA^* + \gamma_4 BB^*B, \quad (1)$$

$$-i\frac{dB}{d\xi} = \gamma_5 BB^*B + \gamma_4 BBA^* + 2\gamma_4 ABB^* + 2\gamma_3 ABA^* + \gamma_3 AAB^* + \gamma_2 AA^*A, \quad (2)$$

where  $A$  and  $B$  denote the amplitudes of the fundamental and XPW, respectively [see Fig. 1(a)].

$\gamma$  coefficients for both cuts are summarized in Table I.  $\beta$  is the angle between input polarization and the crystal axis  $x$ . We note that the characteristic symmetry for  $z$ -cut  $\gamma$  coefficients:  $\gamma_5 = \gamma_1$  and  $\gamma_4 = -\gamma_2$  is broken for the holographic cut orientation. The last line in the Table I gives the orientations of input polarization  $\beta_{\text{zero}}$  for which the XPW signal is zero. These angles, derived from  $\gamma_2(\beta) = 0$ , are different for the two cuts and this can be used to test the correct orientation of the [011]-cut sample.

We solve the system (1) and (2) with initial conditions  $A(\xi=0) = A_0$  and  $B(\xi=0) = 0$ . On Fig. 1(b) we compare the theoretical plane wave efficiencies and demonstrate that the holographic cut yields higher efficiency. The theoretical predictions for XPWG efficiency as a function of the angle  $\beta$  are shown in Figs. 1(c) and 1(d) for both cuts at three different input intensities. For the angle range  $\beta = 0 \dots \pi$ , the maxima of XPWG efficiency at low intensity for  $z$ -cut are at  $\beta_{\text{opt}} = m\pi/8$ , with  $m = 1, 3, 5, 7$ . For the holographic cut the two main (higher) maxima are at  $\beta_{\text{opt},1,2} = (3/8 - 0.0168)\pi$ ;  $(5/8 + 0.0168)\pi$ . As can be seen in Fig. 1(c) the difficulty with the  $z$ -cut is that the angle  $\beta_{\text{opt}}$  changes when the intensity increases. The necessity of  $\beta$  tuning with the change in input intensity increases the experimental complexity in applications where, in order to avoid any parasitic self phase modulation effects in air, the NLC is placed under vacuum. For the holographic cut, as seen in Fig. 1(d),  $\beta_{\text{opt}}$  remains unchanged for any realistic change in input intensity. The insensitivity of  $\beta_{\text{opt}}$  to input intensity for [011]-cut scheme is explained by the fact that compared to the  $z$ -cut case the phase matching conditions for optimal phase shift between the two waves ( $\pi/2$ ) are maintained over a bigger range of input intensity [see Fig. 1(b) left scale, thin lines]. This insensitivity also means less distortions of the temporal and spatial shapes. For the curves shown in Fig. 1(d) the increase in efficiency of the [011]-cut over [001]-cut is 27% for  $S = 1$  and  $S = 2$  and 19% for  $S = 3$ , that is connected with the fact that  $\gamma_2(\beta_{\text{opt}})$  for [011]-cut is 1.12 times bigger the

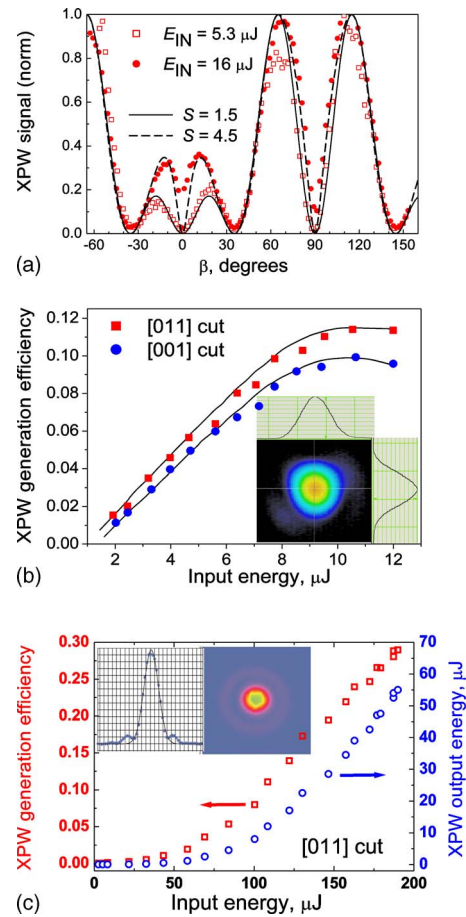


FIG. 2. (Color online) [(a) and (b)] single crystal setup as in Fig. 1(a). (a) XPW signal as a function of angle  $\beta$  for [011] orientation for two different input energies. The lines are theoretical curves (see text). Each of the experimental curves is normalized to the average value of the “highest” three maxima. (b) XPWG efficiencies for the two cuts. The lines are eye guides. Inset: input FB spatial beam shape. (c) XPWG energy (circle) and efficiency (square) for two crystal scheme with two holographic cut  $\text{BaF}_2$  crystals. Inset: output XPW spatial beam shape.

$\gamma_2(\beta_{\text{opt}})$  for [001]-cut. The XPWG efficiencies shown in Figs. 1(b)–1(d) are for plane waves. If the FB has Gaussian spatial and temporal shapes, the energy efficiency is 5 times less,<sup>1</sup> and the amplitude of the oscillations in the energy efficiency curve is reduced. The theoretical prediction for the enhancement in the energy efficiency with the holographic cut compared to the  $z$ -cut is close to 1.3 times.

The NLC used in the experiments are 2 mm thick  $z$ -cut and [011]-cut  $\text{BaF}_2$  crystals. The  $\text{BaF}_2$  sample is placed between two Glan polarizers. Both the  $\text{BaF}_2$  samples and the polarizers are uncoated. The  $\beta$ -dependence measurements were performed with the second harmonic of a colliding-pulse mode-locked (CPM) dye laser (620 nm, 100 fs, 10 Hz). The pulses with an energy up to 20  $\mu\text{J}$  are focused with a  $f = 500$  mm lens into the NLC. Figure 2(a) shows the experimental  $\beta$  dependences of XPWG in the [011]-cut sample. The theoretical curves (lines) for Gaussian/Gaussian shapes for spatial/temporal modulation of the fundamental radiation are obtained by numerically solving the system (1) and (2). The agreement with experiment is very good. The angles  $\beta_{\text{zero}}$  for which the XPW signal is minimal correspond to the values listed in Table I. As predicted, the two main  $\beta$  position maxima for the holographic cut are insensitive to changes in input energy.

The XPWG efficiency measurements were done with a commercial femtosecond laser (Femtolasers GmbH) delivering up to 1 mJ, 30 fs pulses at 1 KHz and  $\lambda=800$  nm. The FB spatial shape is very close to Gaussian, as shown in the inset of Fig. 2(b). The pulse-to-pulse stability of the laser used in the experiment is below 1% ensuring a very small error (3%) in the efficiency measurements. Measured conversion efficiencies (without corrections for losses) for experiment with a single BaF<sub>2</sub> crystal are shown in Fig. 2(b). The pulses are focused with a  $f=0.5$  m lens into the NLC. The efficiency with [011]-cut sample saturates at 11.4%. This value can be compared with the maximum efficiency of 10% reported before with a single crystal.<sup>3,7</sup> Accounting for losses of the output Glan and the NLC, we calculated a 15% internal efficiency. It is very important to note that the efficiency curve for the [001]-cut (circles) in Fig. 2(b) was obtained with reoptimization of angle  $\beta$ , while for experiment with the [011]-cut (squares) such a reoptimization was not necessary as predicted by the model.

As XPW filtering is useful at higher energy in a double CPA scheme, we also tested a two crystals scheme<sup>1,8</sup> for XPWG using two holographic cut BaF<sub>2</sub> crystals. The FB with 7 mm diameter was focused with a  $f=5$  m lens. The two crystals (placed in vacuum chamber) were set  $\approx 50$  cm apart, in accordance with the experimental dependence pointed out in Ref. 9. The obtained XPW energy and efficiency are shown Fig. 2(c). The output spectrum has a near Gaussian shape with 80 nm full width at half maximum (for an input width of 40 nm). The maximum obtained efficiency of 29 % for a 190  $\mu$ J input pulse energy yields a 55  $\mu$ J XPW pulse energy. It is the highest XPW energy efficiency recorded so far with this kind of setup. This value is in fact 1.3 times higher than the previously published values obtained with  $z$ -cut crystals (see Refs. 2 and 8–10), which is in accordance with the prediction of the model. Considering the output pulse shortening obtained via XPWG this result corresponds to a 50% intensity conversion from one polarization to another. Highest efficiencies are obtained for a FB energy

just below the continuum generation threshold.

In conclusion we demonstrate record efficiencies for XPWG using holographic ([011]-cut BaF<sub>2</sub> crystals. We also demonstrate that when [011]-cut crystals are used for XPWG, intensity dependent  $\beta$  compensation of the phase mismatch is not required. This feature makes the holographic cut easier to use for contrast filters in double CPA scheme where the NLC is placed under vacuum. We therefore believe that the use of the holographic cut for XPWG will stimulate the construction of more efficient and more reliable devices for femtosecond pulse contrast improvement.

The support of the contracts LaserLab-Europe, RII3-CT-2003-506350, Extreme Light Infrastructure (Grant No 212105) and Agence Nationale pour la Recherche, through programs BLAN06-3-134072 (ILAR) and Chaire d'Excellence 2004, are gratefully acknowledged. The authors acknowledge the stimulating discussions with B. Mercier, N.M., S.K., and S.S. thank Laboratoire d'Optique Appliquée for their hospitality and support.

<sup>1</sup>A. Jullien, O. Albert, G. Cheriaux, J. Etchepare, S. Kourtev, N. Minkovski, and S. M. Saltiel, *Appl. Phys. B: Lasers Opt.* **84**, 409 (2006).

<sup>2</sup>V. Chvykov, P. Rousseau, S. Reed, G. Kalinchenko, and V. Yanovsky, *Opt. Lett.* **31**, 1456 (2006).

<sup>3</sup>N. Minkovski, G. Petrov, S. M. Saltiel, O. Albert, and J. Etchepare, *J. Opt. Soc. Am. B* **21**, 1659 (2004).

<sup>4</sup>Yu. P. Svirko and N. I. Zheludev, *Polarization of Light in Nonlinear Optics* (Wiley, New York, 1998).

<sup>5</sup>N. Minkovski, S. Saltiel, G. Petrov, O. Albert, and J. Etchepare, *Opt. Lett.* **27**, 2025 (2002).

<sup>6</sup>M. Dabbicco, A. M. Fox, G. von Plessen, and J. F. Ryan, *Phys. Rev. B* **53**, 4479 (1996).

<sup>7</sup>V. M. Gordienko, P. M. Mikheev, and V. S. Syrtsov, *Bull. Russ. Acad. Sci. Phys.* **71**, 122 (2007).

<sup>8</sup>A. Jullien, O. Albert, G. Cheriaux, J. Etchepare, S. Kourtev, N. Minkovski, and S. M. Saltiel, *Opt. Express* **14**, 2760 (2006).

<sup>9</sup>O. Albert, A. Jullien, J. Etchepare, S. Kourtev, N. Minkovski, and S. M. Saltiel, *Opt. Lett.* **31**, 2990 (2006).

<sup>10</sup>A. Cotel, A. Jullien, N. Forget, O. Albert, G. Cheriaux, C. L. Blanc, *Appl. Phys. B: Lasers Opt.* **83**, 7 (2006).